Recent developments in the CTEQ-TEA global analysis: CT18CS and CT18As and Intrinsic Charm in CTEQ-TEA PDFs

Tie-Jiun Hou
侯铁君
University of South China

第二届微扰量子场论研讨会
杭州
Augest 23th, 2022

Global PDF Analysis with Lattice Input

CT18As

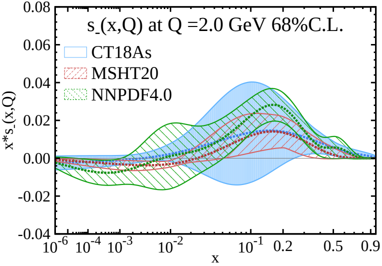

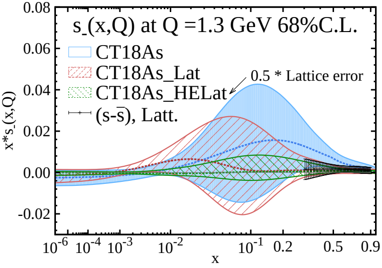

arXiv:2204.07944

CT18CS

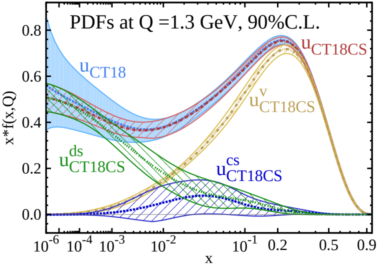

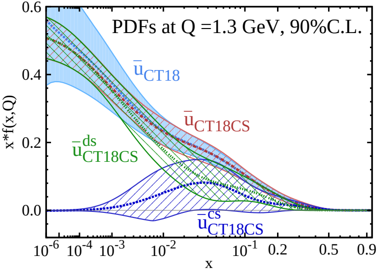

arXiv:2206.02431

CT18 in a nutshell

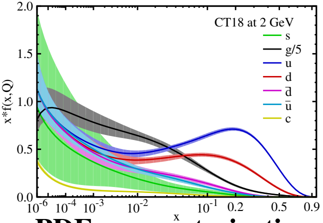

- Start from **CT14-HERAII**:
  (PRD95,034003(2017), T.-J. Hou *et al*)
  HERAII combined data released after publication of CT14
  (PRD93,033006(2016), S. Dulat *et al*).
- Examine a **wide range of non-perturbative PDF parameterizations**.
- Use as much relevant **LHC Run II data** as possible; using applgrid/fastNLO interfaces to data sets, with NNLO/NLO K-factors, or fastNNLO tables in the case of top pair (single and double differential) data.
- Implement a **parallelization** of the global PDF fitting to allow for faster turn-around time.
- Use diverse statistical techniques (**PDFSense**, **ePump**, **Gaussian variables**, **Lagrange Multiplier** scans) to examine agreement between experiments.

PDF Luminosities at 13 TeV LHC
CT18, MMHT20 and NNPDF4.0

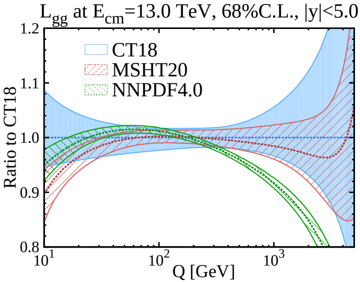

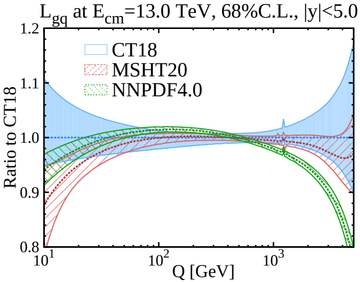

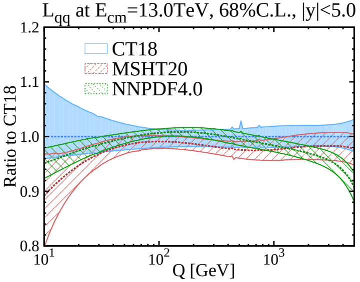

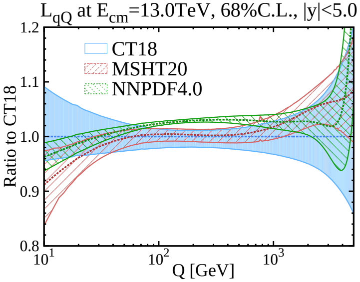

Connected and Disconnected Sea Partons from CT18 Parametrization of PDFs

In Collaborate with Jian Liang, Keh-Fei Liu,
Mengshi Yan, and C.–P. Yuan
arXiv:2206.02431

Gottfried sum rule

Gottfried sum rule (1967) was originally obtain by assuming $\bar{u}$ and $\bar{d}$ to be the same, which leads to

$$S_G = \int_0^1 \frac{dx}{x}\left[F_2^p(x) - F_2^n(x)\right] = \frac{1}{3}, \quad \text{with } \bar{d}(x) \equiv \bar{u}(x)$$

New Muon Collaboration (NMC PRL 66, 2712 (1991), PRD 50, R1 (1994)), $\mu + p(n) \to \mu + X$, obtained

$$S_G = 0.235 \pm 0.026 \quad (\, Q = 2\,\text{GeV}\,)$$

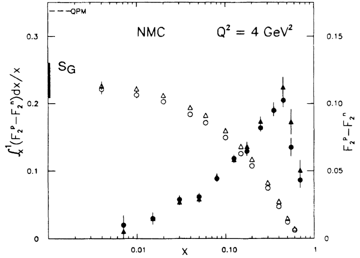

Gottfried sum rule

The alternative expression of Gottfried sum rule is,

$$S_G = \frac{1}{3} - \frac{2}{3}\int_0^1 dx \left(\bar{d}(x) - \bar{u}(x)\right) + O(\alpha_s^2).$$

Hence, NMC data gives

$$\int_0^1 dx \left(\bar{d}(x) - \bar{u}(x)\right) = 0.147 \pm 0.039, \quad \text{at } Q = 2 \text{ GeV}$$

The following experiments like HERMES (PLB387, 419 (1996)) and E866 (PRD64, 052002 (2001)) also shown preference of $\bar{u}/\bar{d}$ flavor asymmetry.

Experiment	$\langle Q^2 \rangle$ (GeV^2)	$\int_0^1 [\bar{d}(x) - \bar{u}(x)] dx$
NMC/DIS	4.0	0.147 ± 0.039
HERMES/SIDIS	2.3	0.16 ± 0.03
FNAL E866/DY	54.0	0.118 ± 0.012

What is the origin of $\int dx \left(\bar{d}(x) - \bar{u}(x)\right) \neq 0$?

Hadronic tensor in Euclidean path-integral formalism

Motivated by Hadronic tensor in QCD path-integral formalism in Euclidian space.

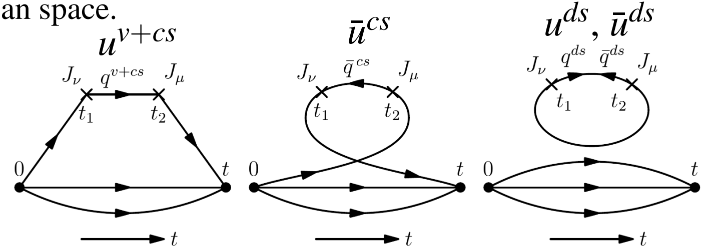

Connected sea(CS) Disconnected sea(DS)

$$
\begin{aligned}
u &= u^{v+cs} + u^{ds}, \quad & d &= d^{v+cs} + d^{ds} \\
\bar{u} &= \bar{u}^{cs} + \bar{u}^{ds}, \quad & \bar{d} &= \bar{d}^{cs} + \bar{d}^{ds}
\end{aligned}
$$

Define $u^v \equiv u^{v+cs} - \bar{u}^{cs}$, which is equivalent to defining $u^{cs} \equiv \bar{u}^{cs}$.

$$
\begin{aligned}
u - \bar{u} &\equiv (u^{v+cs} + u^{ds}) - (\bar{u}^{cs} + \bar{u}^{ds}) = u^v + (u^{ds} - \bar{u}^{ds}) \\
&\neq u^v, \quad \text{unless } u^{ds} = \bar{u}^{ds}
\end{aligned}
$$

Similarly, $d^v \equiv d^{v+cs} - \bar{d}^{cs}$.

Lattice input to global fitting of PDFs

Lattice result from overlap on $N_f = 2+1$ DWF on 4 lattices, with one at physical pion mass (J. Liang *et al*, χQCD, PRD, arXiv:1901.07526)

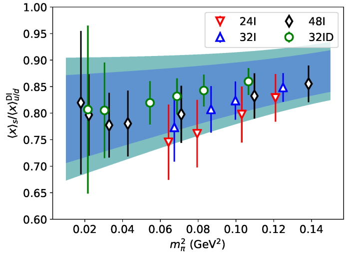

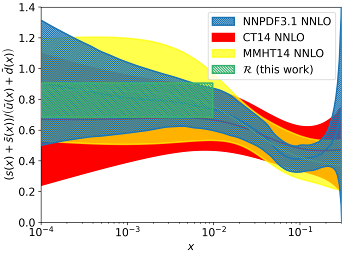

$$\frac{1}{R} = \frac{\langle x \rangle_{s+\bar{s}}}{\langle x \rangle_{\bar{u}+\bar{d}}(DI)} (\text{at } 1.3 \text{ GeV}) = 0.822(69)(78)$$

With this input from Lattice calculation, we assume

$$u^{ds} = \bar{u}^{ds} = d^{ds} = \bar{d}^{ds} = R = R\bar{s},$$

Parton degrees of freedom at $Q_0 = 1.3$ GeV

If we define $u^{cs} \equiv \bar{u}^{cs}$ and $d^{cs} \equiv \bar{d}^{cs}$, the physical parton degrees of freedom used in CT18CS are then:

In CT18

$$
\begin{aligned}
g &= g_{par} \\
u^v &= u^v_{par} \\
d^v &= d^v_{par} \\
\bar{u} &= \bar{u}^{cs} + \bar{u}^{ds} = \bar{u}_{par} + Rs_{par} \\
\bar{d} &= \bar{d}^{cs} + \bar{d}^{ds} = \bar{d}_{par} + Rs_{par} \\
s &= \bar{s} = s_{par}
\end{aligned}
$$

In CT18CS

The non-perturbative PDF functions are further chosen so that

1. $\bar{d}/\bar{u} \xrightarrow{x\to 0} 1.$ $\Leftarrow$ Isospin symmetry, similar to CT18
2. $\bar{u}^{ds}, \bar{d}^{ds}, \bar{s}^{ds} \xrightarrow{x\to 0} x^{-1}.$ $\Leftarrow$ Similar to CT18
3. $\bar{u}^{cs}, \bar{d}^{cs} \xrightarrow{x\to 0} u^v, d^v.$ $\Leftarrow$ $\bar{q}^{cs}$ is in the connected insertion
4. $d/u \xrightarrow{x\to 1} d/u$ of CT18. $\Leftarrow$ Valence behavior, similar to CT18.
5. $\bar{d}/\bar{u} \xrightarrow{x\to 1} \bar{d}/\bar{u}$ of CT18. $\Leftarrow$ Describe E866 and E906 data.

CT18CS PDFs

With the input of $\bar{u}^{ds} = \bar{d}^{ds} = Rs^{ds}$, and

$$\frac{1}{R} \equiv \frac{\langle x \rangle_{s+\bar{s}}}{\langle x \rangle_{\bar{u}+\bar{d}}(DI)} = 0.822 \,\text{at}\, 1.3 \text{ GeV}$$

from lattice QCD, and considering the ansatzs of small-x behavior, we obtain the CT18CS at $Q_0 = 1.3$ GeV scale.

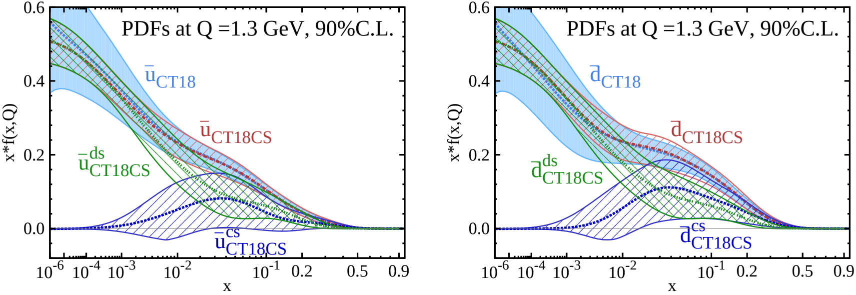

CT18CS PDFs

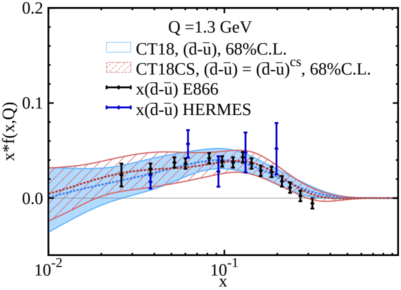

Q =1.3 GeV
CT18, (d̄-ū), 68%C.L.
CT18CS, (d̄-ū) = (d̄-ū)^cs, 68%C.L.
x(d̄-ū) E866
x(d̄-ū) HERMES
x*f(x,Q)
x

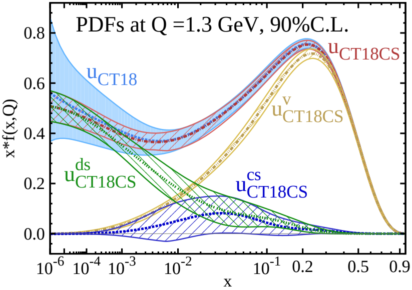

PDFs at Q =1.3 GeV, 90%C.L.
u_CT18
u_CT18CS
u^v_CT18CS
u^ds_CT18CS
u^cs_CT18CS
x*f(x,Q)
x

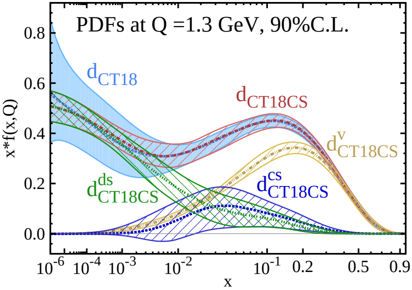

PDFs at Q =1.3 GeV, 90%C.L.
d_CT18
d_CT18CS
d^v_CT18CS
d^ds_CT18CS
d^cs_CT18CS
x*f(x,Q)
x

The $\langle x \rangle$ Moment of CT18CS at 1.3 GeV

The $\langle x \rangle$ moment of CT18 and CT18CS at 1.3 GeV:

PDF	$<x>_{u^v}$	$<x>_{d^v}$	$<x>_g$	$<x>_{\bar{u}}$	$<x>_{\bar{d}}$	$<x>_s$
CT18	0.325(5)	0.134(4)	0.385(10)	0.0284(22)	0.0361(27)	0.0134(52)
CT18CS	0.323(4)	0.136(3)	0.384(12)	0.0287(25)	0.0364(34)	0.0137(39)

PDF	$<x>_{u^{v+cs}}$	$<x>_{d^{v+cs}}$	$<x>^{\star}_{\bar{u}^{cs}}$	$<x>^{\star}_{\bar{d}^{cs}}$	$<x>^{\S}_{u^{ds}}$
CT18CS	0.335(7)	0.155(8)	0.0120(64)	0.0197(70)	0.0167(49)

More direct comparison between global analysis and lattice calculation can be done for each parton degree of freedom, instead of being limited to $u-d$ and s.

	$Q = 2.0$ GeV CT18	Lattice	$Q = 1.3$ GeV CT18CS	CT18
$\langle x \rangle_{u^+-d^+}$	0.156(7)	$0.111-0.209^{N_f=2+1}$ $0.153-0.194^{N_f=2+1+1\dagger}$ $0.166-0.212^{N_f=2}$	0.173(7)	0.175(8)
$\langle x \rangle_{s^+}$	0.033(9)	$0.051(26)(5)^{\ddagger}$	0.027(8)	0.027(10)

† Prog. Part. Nucl. Phys., 121:103908, 2021. ‡ Phys. Rev. Lett., 121(21):212001, 2018

$$u^+ - d^+ = (u+\bar{u}) - (d+\bar{d}) = (u^{v+cs} + u^{ds} + \bar{u}^{cs} + \bar{u}^{ds}) - (d^{v+cs} + d^{ds} + \bar{d}^{cs} + \bar{d}^{ds})$$

$$\xrightarrow{CT18CS} (u^{v+cs} - d^{v+cs}) + (\bar{u}^{cs} - \bar{d}^{cs})$$

$$s^+ = s + \bar{s} = s^{ds} + \bar{s}^{ds} \xrightarrow{CT18CS} 2s^{ds}$$

Summary

- PQCD and LQCD are both important methods for studying the structure of hadron. But there were only few physical quantities can be used for comparison is the past.

- With the input from lattice QCD, $\frac{1}{R} \equiv \frac{\langle x \rangle_{s+\bar{s}}}{\langle x \rangle_{\bar{u}+\bar{d}}(DI)}$, we consider global analysis with the connected sea parton degrees of freedom taken into account, which are respondsible for $\bar{u} \neq \bar{d}$, as suggested by data. The result of global analysis, the CT18CS, is found to be compatible with CT18.

- The CT18CS allows to provide direct comparison between lattice calculations and global analysis for each parton degree of freedom.

Impact of lattice $s(x) - \overline{s}(x)$ data in the CTEQ-TEA global analysis

In Collaborate with Huey-Wen Lin, Mengshi Yan, C.-P. Yuan
arXiv:2204.07944

CT18 with $s(x) \neq \bar{s}(x)$

In the framework of CT18, 6 d.o.f of partons are parametrized at $Q_0 = m_c = 1.3$ GeV.

$$g, \quad u^v, \quad d^v, \quad \bar{u}, \quad \bar{d}, \quad s.$$

Where $\bar{s}(x) \equiv s(x)$ is assumed. The number sum rule for strangeness is satisfied naively. Because the DGLAP equation preserve

$$\int_0^1 [s(x) - \bar{s}(x)]dx = 0,$$

People used to parametrize the strange as $s_+ = s + \bar{s}$ and $s_- = s - \bar{s}$. For example, in CTEQ 6

$$s_+(x, Q_0) = a_0^s x^{a_1 - 1}(1-x)^{a_2} P_+(x)$$
$$s_-(x, Q_0) = s_+(x, Q_0) \tanh[a x^b (1-x)^c P_-(x)]$$

$$P_-(x) = \left(1 - \frac{x}{x_0}\right)(1 + dx + ex^2 + ...)$$

CT18 with $s(x) \neq \bar{s}(x)$

We consider an alternative way on parametrizing the strangeness. Consider both s and $\bar{s}$ contain an overall factor a_0 :

$$s(x, Q = Q_0) = a_0^s x^{a_1^s - 1}(1-x)^{a_2^s} P^s(x) = a_0^s g^s(x)$$

$$\int_0^1 [a_0^s g^s(x) - a_0^{\bar{s}} g^{\bar{s}}(x)] dx = 0$$

By given $a_0^{\bar{s}}$, the a_0^s can be determined by the strange number sum rule.

$$a_0^s = \frac{\int a_0^{\bar{s}} g^{\bar{s}}(x) dx}{\int g^s(x) dx}$$

- Different from the root-finding method, there is no presumed requirement on the function form of $g^s(x)$ and $g^{\bar{s}}(x)$.
- But it is relatively hard to control the number of crossing in $s - \bar{s}$.

CT18As NNLO:
CT18A with Strangeness Asymmetry

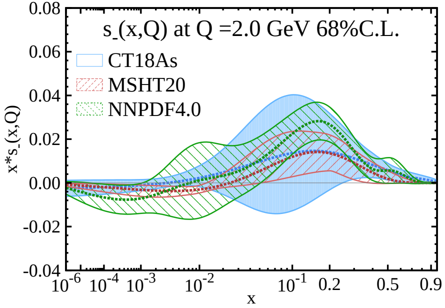

Starting from CT18A, we select the strange asymmetry with single crossing from various trial parametrizations.

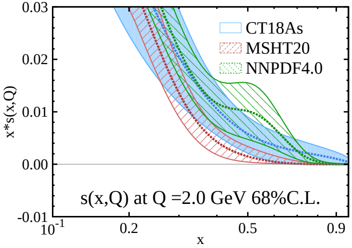

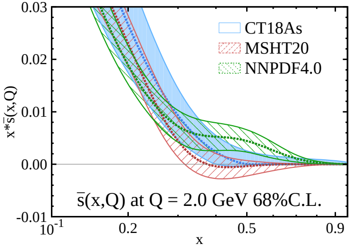

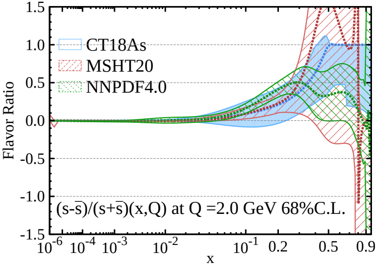

Asymmetry norminally reaches $\sim 50\%$ at $x \sim 0.25$ in three global fits.

$s_- \neq 0$ is preferred by LHC Drell-Yan processes and E866 p/d ratio.

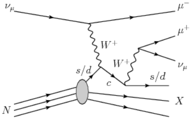

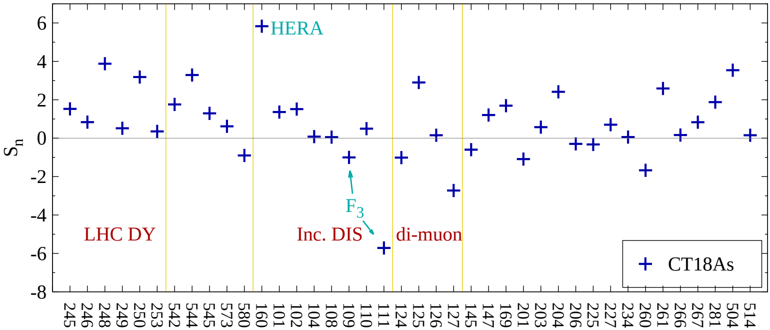

First Lattice Strange PDF

§ On the lattice, one needs to calculate the following

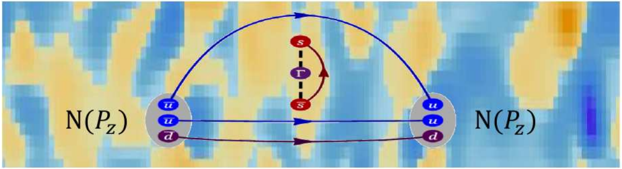

2005.12015, Zhang, Lin, Yoon

§ Results by MSULat/quasi-PDF method

- Clover on 2+1+1 HISQ 0.12-fm 310-MeV QCD vacuum
  - 7,184,000 strange loops
  - 344,832 nucleon correlators
- RI/MOM renormalization
- Extrapolated to $M_\pi \approx 140$ MeV

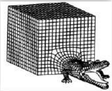

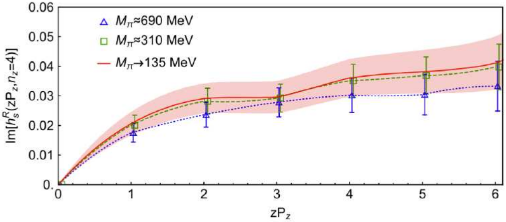

First Lattice Strange PDF

§ Lattice matrix elements

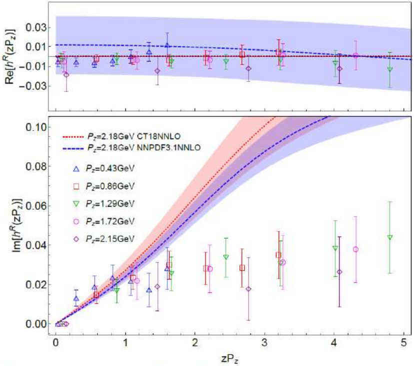

❧ Strange-antistrange symmetry

$$\mathrm{Re}[h(z)] \propto \int dx\,(s(x) - \bar{s}(x))\cos(xzP_z)$$

$$\mathrm{Im}[h(z)] \propto \int dx\,(s(x) + \bar{s}(x))\sin(xzP_z)$$

$s(x) - \bar{s}(x)$

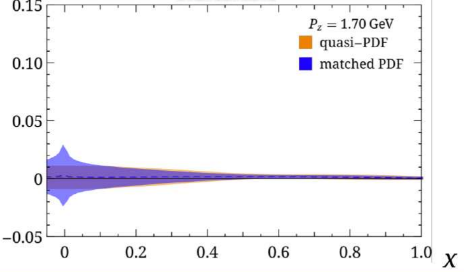

§ From quasi-PDF to PDF

$$\tilde{f}_q(x, P_z) = \int_{-1}^{1} \frac{dy}{|y|} f_q(y) C_{q/q}(x, y, P_z, \mu)$$

$$+O\left(\frac{\Lambda_{QCD}^2}{x^2 P_z^2}, \frac{\Lambda_{QCD}^2}{(1-x)^2 P_z^2}\right)$$

CT18As_Lat:

Strangeness asymmetry with a lattice QCD constraint

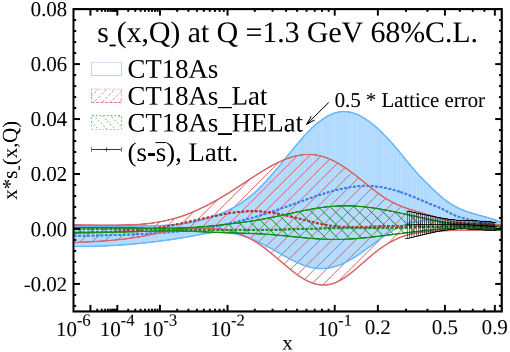

CT18As:
CT18A with strange asymmetry.
CT18As_Lat:
PDFs with lattice input.
CT18As_HELat:
PDFs if the lattice errors are reduced by 1/2.

- Lattice QCD calculation provide prediction for $0.3 < x < 0.8$.
- Lattice QCD prediction disfavors a large $s_-(x,Q)$ for $x > 0.3$ region. It cause the reduction in $s_-(x,Q)/s_+(x,Q)$ for $x < 0.3$ (depending on the parametrization form).

CT18As_Lat:
Strangeness asymmetry with a lattice QCD constraint

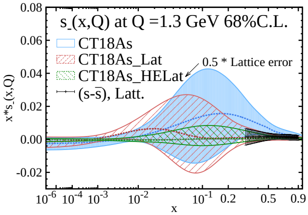

Di-muon data provide measurments for $0.015 < x < 0.336$.

DIS and dimuon SIDIS show less clear trends.

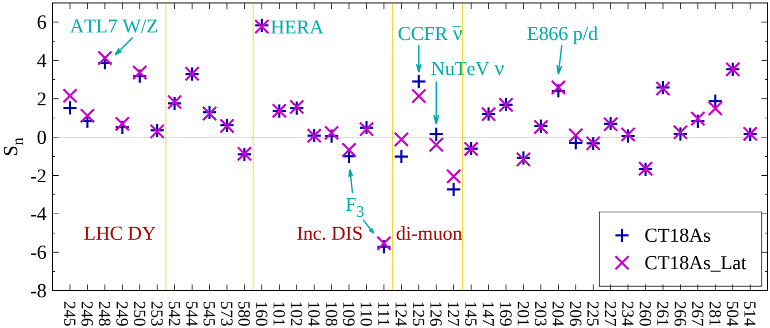

Summary

- Lattice QCD calculation disfavors a large $s_-(x, Q)$ for $x > 0.3$.
- By treating lattice QCD calculation as data, we have chance to determine PDFs at $x \to 1$.
- The framework of global analysis provide indirect comparsion between lattice calculations and experimental measurements in the overlap region.

Intrinsic Charm in CTEQ-TEA PDFs
CT14 IC: answers to important questions

What are phenomenological constraints on the ”intrinsic charm” from the global QCD data?

$\Rightarrow$ The CT14 charm PDFs allow a ”nonperturbative” component carrying a total momentum fraction of $1-2\%$ in DIS at $Q \sim m_c$.

Can we estimate its impact on the LHC predictions?

Yes, based on the simplest approximation of the ”nonpertubative” charm contribution. In most cases, the estimated impact is less then the net CT14 PDF uncertainty.

Hou et al., JHEP 02(2018)059, arXiv: 1707.00657

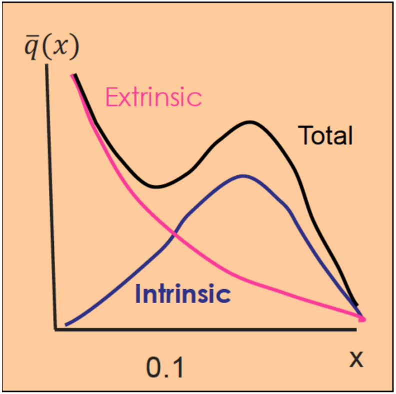

Instead of parametrize the charm as strange in the usual way, we concern the possibility of **valence-like**(intrinsic) and **sea-like**(extrinsic) component of charm.

1.The Sea-like(extrinsic) component:

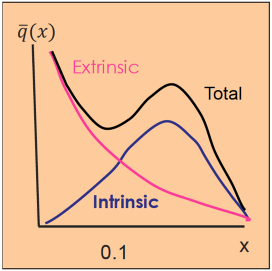

- Monotonic in x, satisfies

$$q(x) \propto x^{-1}, \text{ for } x \to 0$$

- May be generate in several ways, e.g.

  In PQCD, from gluon splittings

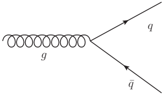

  In Lattice QCD, from disconnected diagrams

2.Valence-like (intrinsic) component:

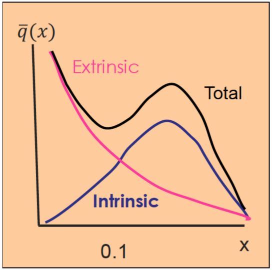

- peaks in x, satisfies

$$q(x) \propto x^{-1/2}, \text{ for } x \to 0$$

- May be generate in several ways, e.g.

  For all flaovers, nonperturbatively from a $|uudQ\bar{Q}>$ Fock state.
  (Brodsky, Peterson, Sakai, PRD 1981)

  In Lattice QCD, from connected diagrams

Parametrizations of $c(x, Q_0)$

- "**Valence-like**" $c(x, Q_0)$ according to the BHPS model: (Brodsky et al, PLB 1980)

$$c(x) = \bar{c}(x) = \frac{1}{2} A\, x^2 \left[\frac{1}{3}(1-x)(1+10x+x^2) - 2x(1+x) \ln(1/x) \right].$$

- "BHPS3" model: we include intrinsic $u\bar{u}$, $d\bar{d}$ and $c\bar{c}$ with **numerical** solutions for the BHPS model.

- "**Sea-like**" $c(x, Q_0)$:

$$c(x) = \bar{c}(x) = A \left[\overline{d}(x, Q_0) + \overline{u}(x, Q_0) \right]$$

Charm Momentum Fraction

$$\langle x \rangle_{c+\bar{c}}(Q) = \int_0^1 x\,[c(x,Q) + \bar{c}(x,Q)]\,dx$$

Initial scale $Q_0 \leq m_c$, intrinsic component only

$$\langle x \rangle_{\text{IC}} = \langle x \rangle_{c+\bar{c}}(Q_0)$$

At $Q > Q_0$, growth due to perturbative $c(x,Q)$

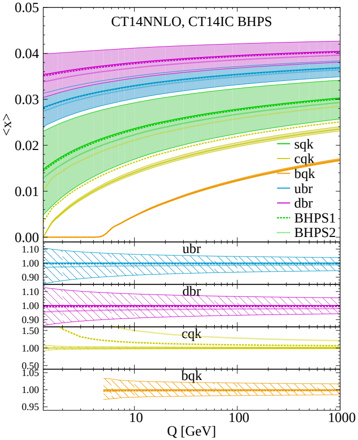

Setup for the global analysis for CT14 and CT14HERA2:

- $\alpha_s(M_Z) = 0.118$, compatable with the world average value $\alpha_s(M_Z) = 0.1184 \pm 0.0007$; the default value for recent CT PDF fits. Different value of $\alpha_s(M_Z)$ yields different PDFs.

- HOPPET - evolution code used to include nonperturbative charm model with NNLO matching, and to evolve the PDF at NNLO.

- Partons are parametrized at the initial energy scale $Q_0 = 1.295$GeV, which is slightly lower than the default charm quark mass $m_c^{pole} = 1.3 GeV$.

- Choose experimental data with $Q^2 > 4$ GeV^2 and $W^2 > 12.6$GeV^2 to minimize high-twist, nuclear correction, etc., and focus on perturbative QCD predictions.

Difference in CT14HERA2 from CT14:

- Combined HERA Run I+II data were used in place of the HERA Run I data in CT14.
- One of the poorly fit NMC data were drop in CT14HERA2.
- Strange quark no longer bound with $\bar{u}$ and $\bar{d}$. Smaller strangeness is prefer than CT14.
- More geneal model BHPS3 use the setup of CT14HERA2.

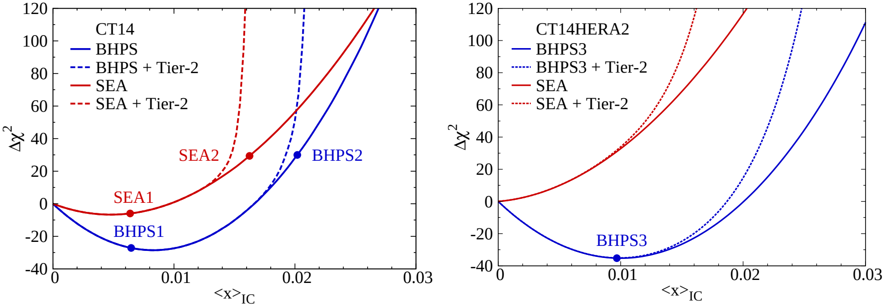

For 90% C.L.,

$$\langle x \rangle_{\rm IC} \lesssim 0.021 \text{ for CT14 BHPS,}$$
$$\langle x \rangle_{\rm IC} \lesssim 0.024 \text{ for CT14HERA2 BHPS,}$$
$$\langle x \rangle_{\rm IC} \lesssim 0.016 \text{ for CT14 and CT14HERA2 SEA.}$$

Impact of IC on the PDFs and their ratios

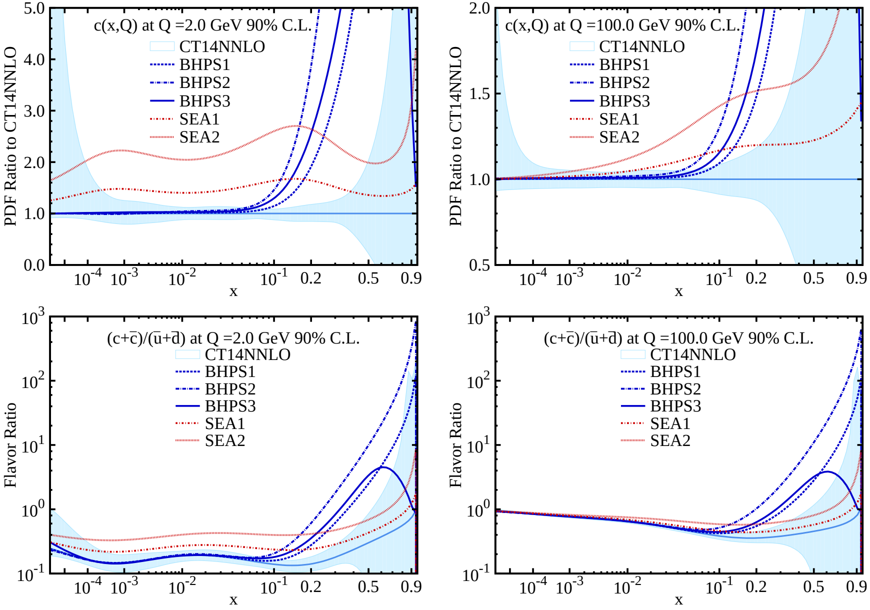

CT18IC PDFs

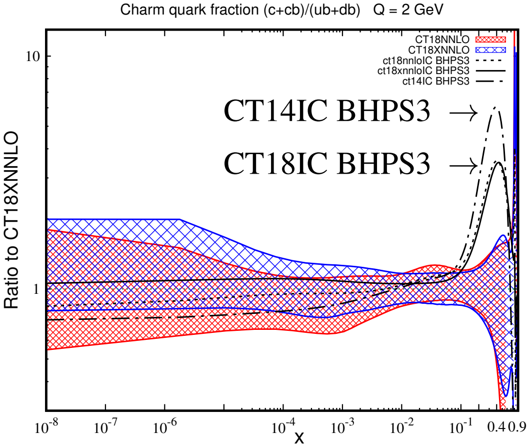

With the inclusion of LHC RUN II data, the CT18IC BHPS 3 shows lower Brodsky peak.

Guzzi et al., SciPost Phys.Proc. 8 (2022) 005, arXiv: 2108.06596

Dependence of Fit on the Charm-Quark Mass

The combined HERA charm production and inclusive DIS data play an important role in the description of the goodness of fit. m_c is a key input scale.

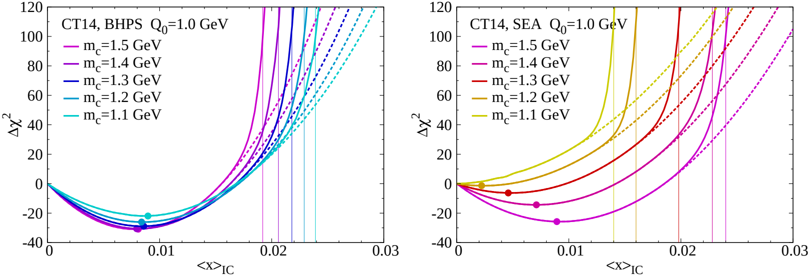

BHPS model: the position of the χ^2 minimum is relatively stable as m_c is varied, while the upper limit on the amount of IC decreases to 1.7%. BHPS model is not dramatically affected by variations of m_c

SEA model: limits on the amount of IC allowable are shifted towards higher values. ubar and dbar are well constrained by data (vector boson production in pp and pbar p) in the intermediate/small x region, and cannot change too much

European Muon Collaboration (EMC)

Semi-inclusive dimuon and trimuon production in DIS on an iron target

- Excess in a few high-x bins of the $F_{2c}(x, Q)$
- No systematic error.
- Analysis done at the leading order of QCD.
- Tension with various inclusive and semi-inclusive DIS data.

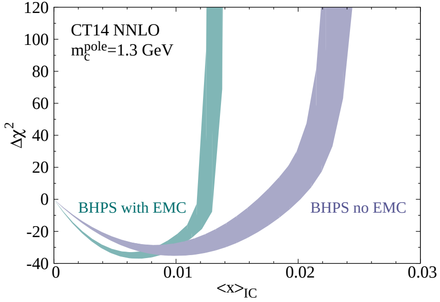

J. J. Aubert et al. (European Muon Collaboration), Nucl. Phys. B213, 31 (1983).

LHC: NNLO Total inclusive electroweak boson production cross sections $\sigma_{tot}(pp \to VX)$

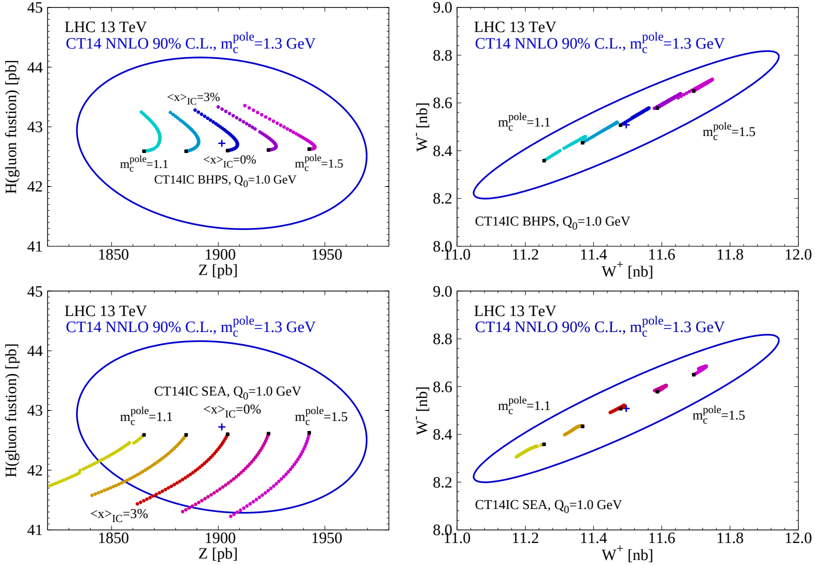

LHC Searches for Intrinsic Charm

Z+c NLO computation with various models, without (left) and with parton shower (right)

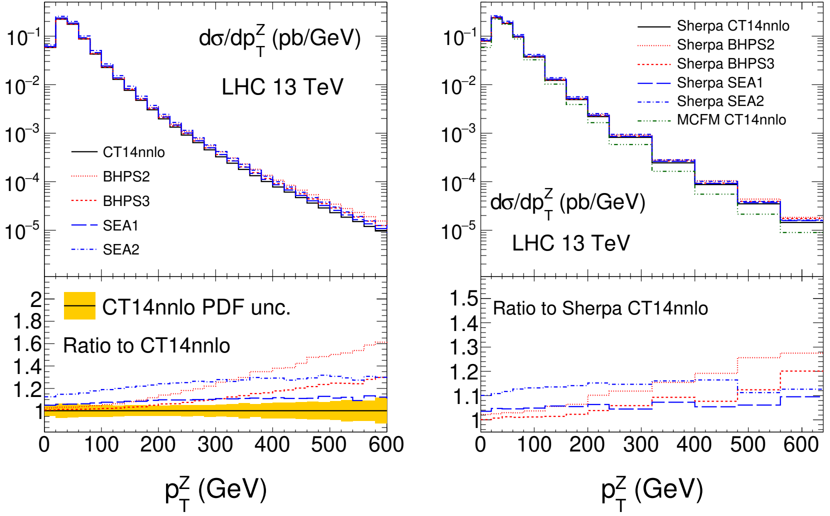

LHCb Z+c

LHCb provide measurement of Z+c at 13 TeV with 6 fb^{-1} for $2.0 < y(Z) < 4.5$. (Phys.Rev.Lett. 128 (2022) 8, 082001 [arXiv: 2109.08084])

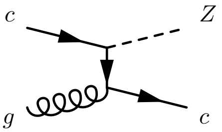

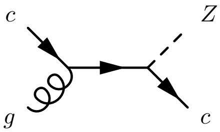

CT14IC BHPS3 with $\langle x \rangle_{IC} = 1\%$ can explain the excess in the high $y(Z)$ bin in LHCb Z+c data.

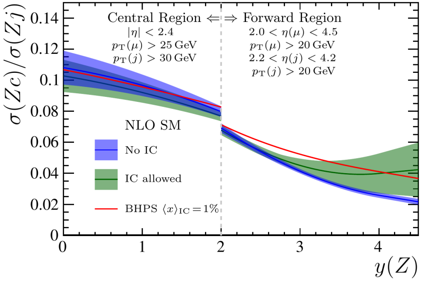

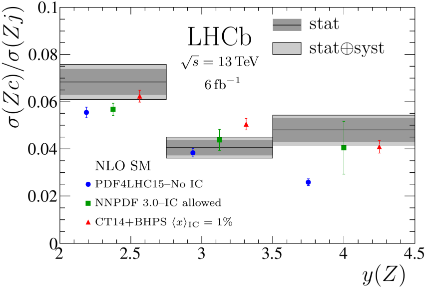

EIC, charm production

Orders-of-magnitude more events for some IC models

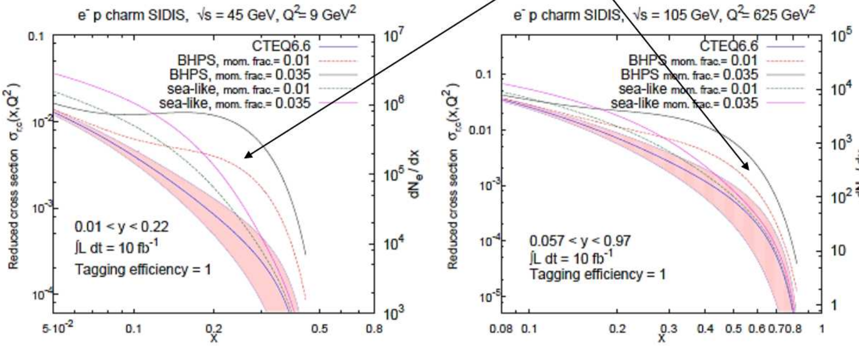

Figure 1.20. Charm contribution to the reduced NC e^-p DIS cross section at $\sqrt{s} = 45$ and 105 GeV. For each IC model, curves for charm momentum fractions of 1% and 3.5% are shown. For comparison we display the number of events dN_e/dx for $10\,\mathrm{fb}^{-1}$, assuming perfect charm tagging efficiency.

[Guzzi, Nadolsky, Olness, in arXiv:1108.1713; see also T. Hobbs, arXiv:1707.06711]

Summary

- Intrinsic charm was estimated in the framework of CT14 and CT18 by using valence-like BHPS model and sea-like model.

- Best fit of CT14IC with $\langle x \rangle_{\mathrm{IC}} \sim 1\%$, the CT14IC BHPS 3 PDF, was presented which is not sensitive to the choice of m_c.

- The LHCb Z+c data has good agreement with CT14IC in high $y(z)$ bin.

Thank you
for your attention